ESTIMATION OF FLOW-INDUCED LOADS ON A DOWN-SCALED MODEL OF SMART REACTOR COOLANT SYSTME

Kyoung Rean Kim[1], Jin Seok Park[1] and Won Jae Lee[1]
[1] SMART Development Department, Korea Atomic Energy Research Institute, 1045 Daedeok-daero, Yuseong, Daejeon 305, Republic of Korea
kimkr1@kaeri.re.kr, khjeong@kaeri.re.kr, jspark1@kaeri.re.kr, wjlee@kaeri.re.kr

Abstract

SMART (System-integrated Modular Advanced Reactor) is a small and medium-sized integrated reactor to produce an electric power and desalination simultaneously. SMART should be designed to withstand flow-induced loads generated by the coolant flow under both normal and transient operations during the design period. In this study, we evaluated the flow-induced loads and flow characteristics in the axial and the circumferential directions of reactor internals using a down-scaled model of SMART prototype. This paper shows that the simulated results in the axial direction are in good agreement with the experimental data in the reactor coolant system. The flow-induced loads are irregularly distributed in the circumferential direction of the reactor internals.

1. Introduction

SMART (System-integrated Modular Advanced Reactor) is a small and medium-sized integrated reactor to produce an electric power and desalination simultaneously. SMART consists of reactor internals, reactor vessel and major components such as reactor coolant pumps, steam generators, and control rod assemblies. The major components and the reactor internals should be designed to withstand flow-induced loads generated by the coolant flow under either normal or transient operations during the design period. The coolant flow between the reactor internals and the major components produces the flow-induced loads and eventually it can induce vibrations of the structures[1-2]. Therefore, it is necessary to estimate the coolant flow loads in the normal and transient operation.

Much time and cost could be needed to get the flow-induced loads on the reactor internals by the hydraulic test with SMART prototype. Therefore, this study intends to evaluate the flow-induced loads and flow characteristics using the down-scaled model having the similarities of SMART prototype. The down-scaled model was designed with one tenth-size of the SMART prototype.

The flow-induced loads in the axial and circumferential directions of reactor internals were calculated by using a commercial fluid dynamic software, FLUENT. The flow-induced loads of CFD analysis result were compared with the experimental result[3] in the entire region inside the down-scaled model.

2. Down-scaled model for SMART prototype

The down-scaled model is used to evaluate the flow-induced loads on the reactor internals. It consists of the reactor, steam generator, flow mixing header, flow skirt, core part, upper guide structure, core support barrel assembly and various pipes as shown in figure 1[3].

Most components of the down-scaled model are same shaped in SMART prototype. Steam generator in the down-scaled model is simulated with many orifice plates for pressure loss. The core part in the down-scaled model is simulated with many orifice plates for pressure loss characteristics.

Figure 2 shows the measurement locations of the static pressure sensors to identify axial pressure distribution. Eleven units of the static pressure probe for measuring the pressure distribution are installed on the wall of the down-scaled model[3]. The numbering order of the static pressure probes are defined based on the horizontal direction starting from the pipe inlet.

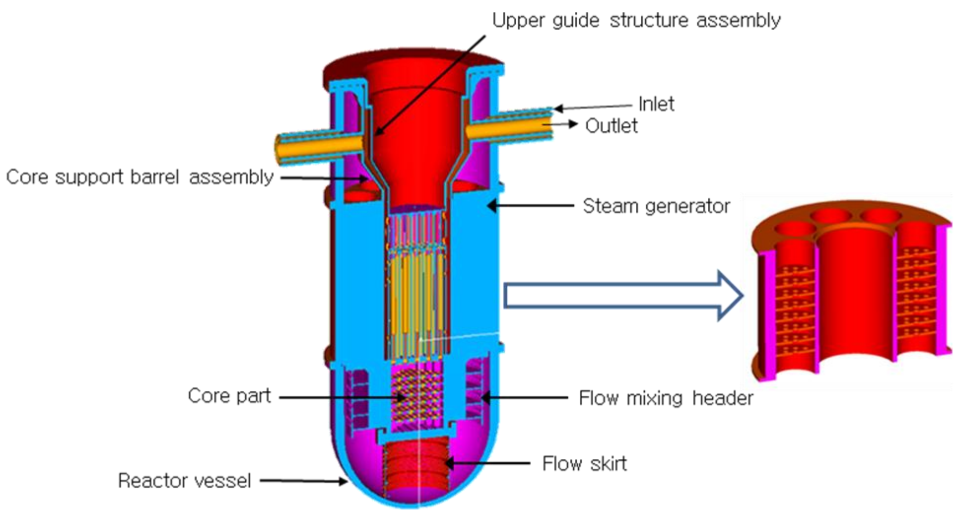

Figure 1 Schematic model of down-scaled model for SMART prototype

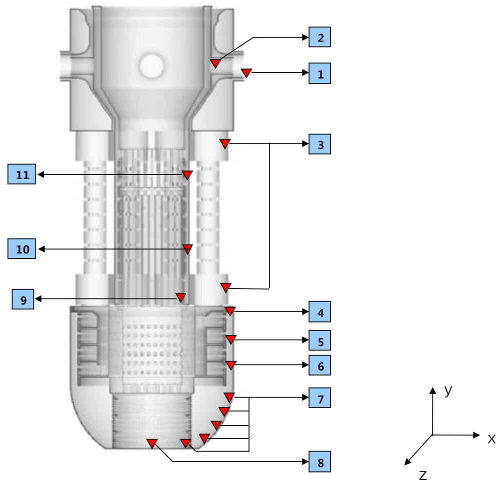

Figure 2 Pressure measurement locations in the down-scaled model

3. Computational fluid dynamic analysis

3.1 Analysis method and boundary condition

We use FLUENT program to calculate the flow-induced load in the down-scaled model of SMART prototype. FLUENT is an analysis program which can be used to calculate the incompressible, compressible and transonic flow.

Figure 3 shows the computational domain for the flow-induced load evaluation of the down-scaled model. The mesh size is about 32,400 thousand cells for the computational model(95% of structured mesh and 5% of unstructured mesh). The structured mesh(Hexahedral element) is used at most of the computational area such as upper reactor vessel, steam generator, flow mixing header, flow skirt, reactor vessel, core part, upper guide structure assembly and core support barrel assembly. Unstructured mesh(Tri-element) is used at the complicated regions like the control rod shroud tube and lower support plate of the upper guide structure assembly. The small sized mesh is generated on the wall of reactor vessel and flow mixing header because of turbulence and vortex shedding calculation[4].

In this paper, the turbulence model adopted in the steady state simulation is the realizable k-ε which is used to enclose the governing equations. It is generally used to apply the complicated geometry. The density of the water is 998.2 kg/m^3 and viscosity of the water is 0.001003 kg/m-s at room temperature and atmosphere pressure[5]. Inlet boundary condition for CFD analysis is determined as flow rate. Outlet condition is assumed at atmosphere pressure for CFD analysis.

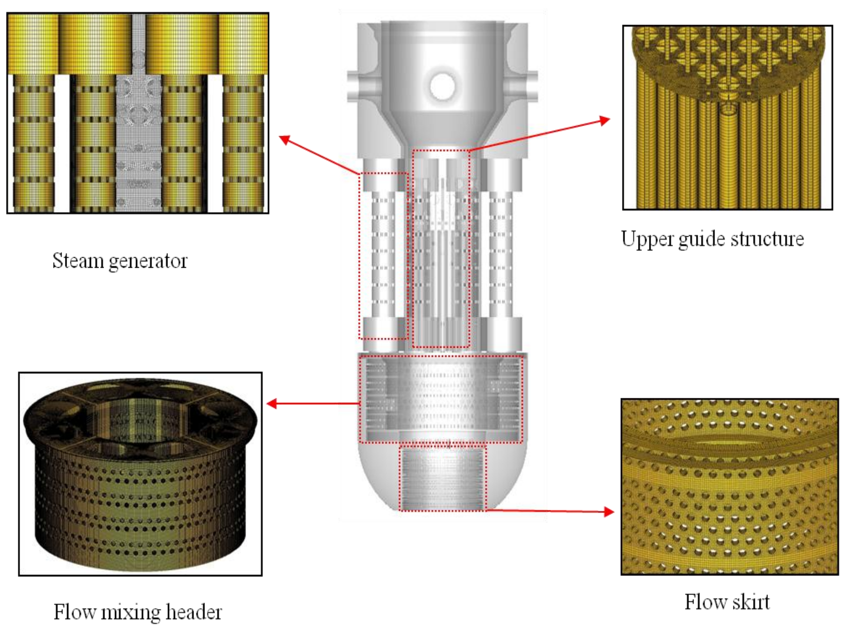

Figure 3 Computational meshes for down-scaled model

3.2 Axial pressure distribution of the reactor coolant system

The down-scaled model for SMART prototype is equipped with the pump to circulate the fluid in the reactor coolant system. The fluid flows into the upper part of reactor vessel through an inlet pipe by the operation of the pump. The internal structure of the reactor and major components are influenced by the flow-induced loads created by the flow of the fluid. The flow-induced loads can be obtained through the pressure distribution of the axial direction generated inside reactor coolant system.

Figure 4(a) shows the comparison of experimental result[3] and flow analysis result in the entire region inside the down-scaled model. The axial pressure distribution of reactor coolant system appeared to be identified between the experimental data and the analysis result. The fluid at the inlet strongly collided to the wall of the upper part reactor vessel but the pressure loss did not largely occur. Steam generator and core part have the biggest pressure loss in the reactor coolant system as shown in figure 4(a). At the steam generator and the core part, the momentum of the fluid decreased because of the complicated shape and the influence of the perforated plate.

The average error between the experimental data and the analysis result occurred about 5% in the most of area, however about 8% of error appeared at the upper part of the core support barrel due to the complicated shape. The axial pressure distribution of the reactor coolant system declines proportionally as the flow rate decreases.

Figure 4(b) is the axial pressure distribution generated at the down-scaled model when considering the pressure generated by the water head. The axial pressure distribution increases with the direction of the fluid flow inside the down-scaled model, and sharply decreases as passing the flow skirt. When the fluid flows downward (the gravity direction), the pressure distribution by the water head increases more than the pressure loss generated inside the down-scaled model. When the fluid flows upward (the opposite direction of gravity), the axial pressure distribution decreases by the pressure loss and water head decrease generated inside the down-scaled model.

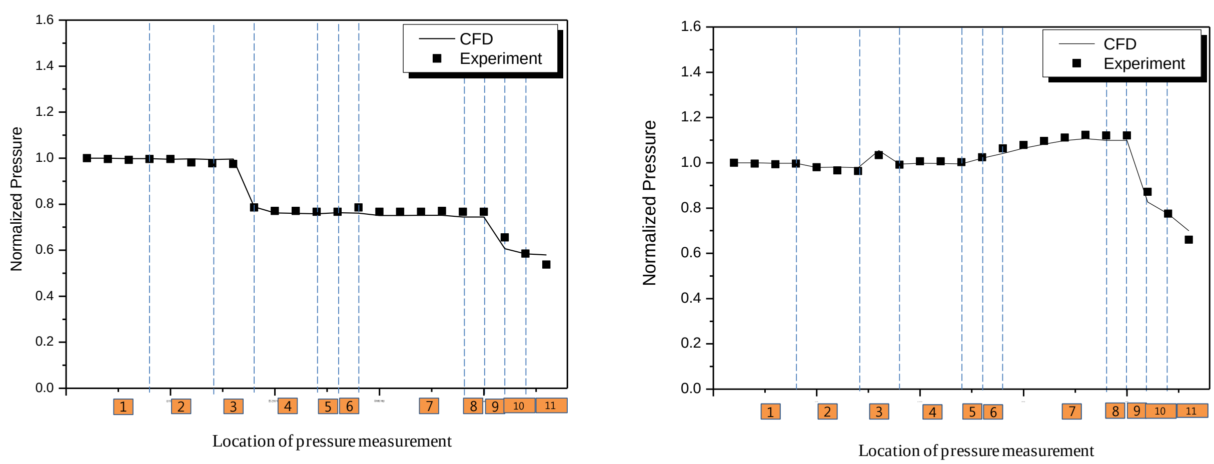

(a) without the pressure head **(b) with the pressure head**

Figure 4 Pressure distribution in the axial direction of the down-scaled model

3.3 Circumferential of the reactor coolant system

In this section, the circumferential pressure distribution displayed by fluid circulating inside the down-scaled model is described.

Figure 5 is the circumferential pressure distribution at the outside wall of the core support barrel and the inside wall of the upper part of the reactor vessel. The fluid flowed through the inlet pipe shows a pressure increase of about 400 Pa as colliding at the outside wall of the core support barrel. The fluid flows along the outside wall of the core support barrel and forms the secondary flow as being combined at the 45˚, 135˚, 225˚, 315˚ location. At these locations, the pressure increases by about 300 Pa because of the secondary flow.

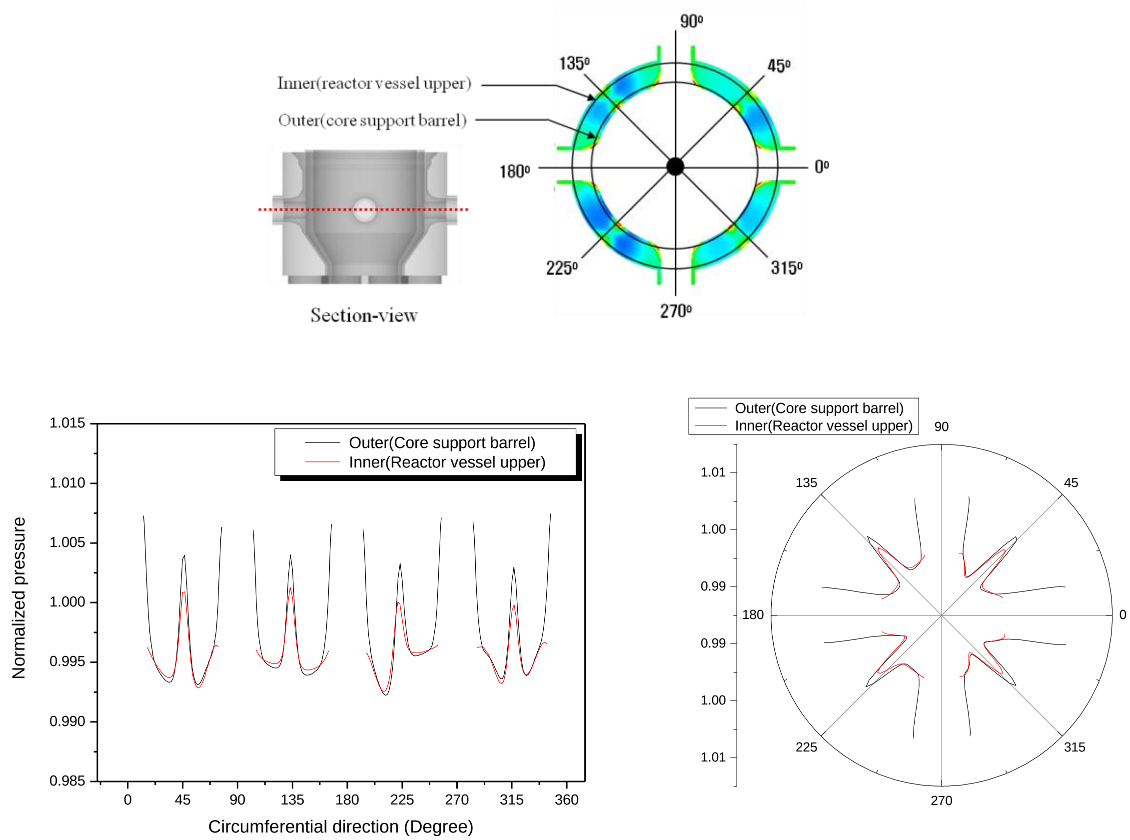

Figure 5 Pressure distribution in the circumferential direction of the reactor vessel upper and core support barrel

Figure 6 is the circumferential pressure distribution at the inside wall of the upper part of the reactor vessel and the outside wall of the core support barrel. The fluid flows to the steam generator after mixing at the upper part of the reactor vessel. The circumferential pressure distribution difference before flowing into the inside of the steam generator was about 80Pa. The circumferential pressure distribution difference was decreased as about 4 times as the pressure distribution generated at the upper part of the reactor vessel. At the entry part of the upper part of steam generator, the flow velocity increases because the flow area is decreased by the structure.
Figure 7 is the circumferential pressure distribution generated inside the flow skirt and the wall of the lower part of the reactor vessel. The fluid collides to the lower wall of the reactor vessel through the perforated plate of the flow mixing header. It is noticed that the pressure distribution is irregularly formed as shown in this Figure 7. The irregular fluid discharged from the flow mixing header becomes uniform by the perforated plate of the flow skirt.

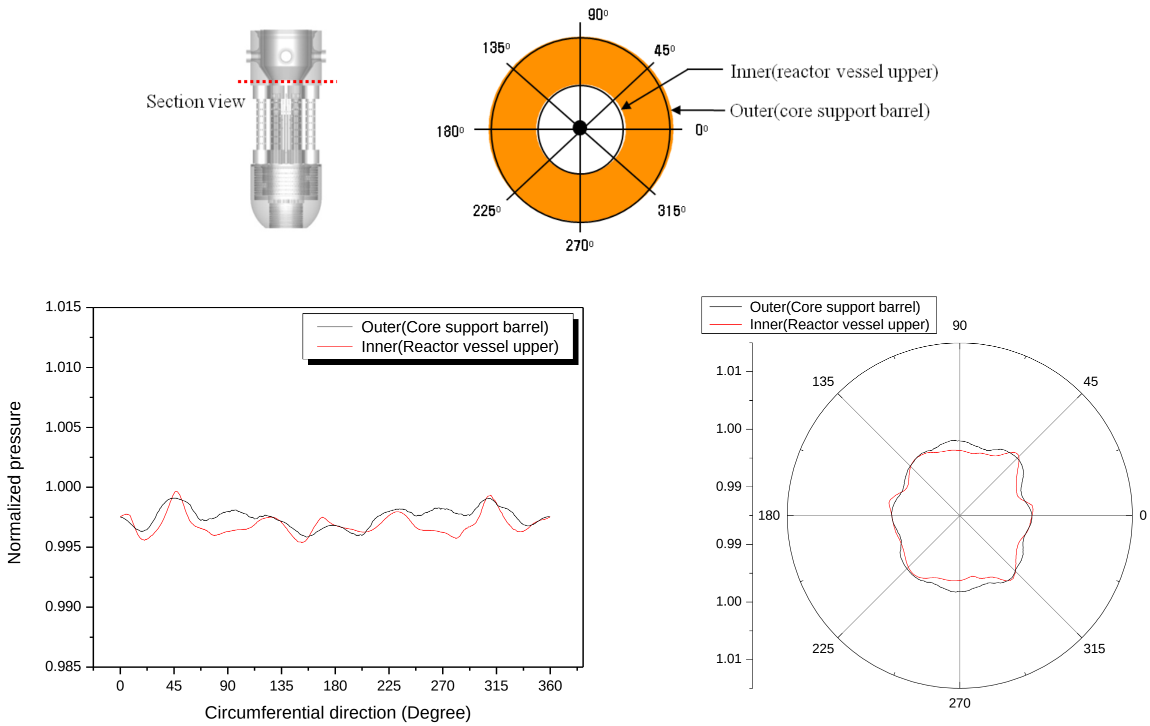

Figure 6 Pressure distribution in the circumferential direction of the reactor vessel upper and core support barrel

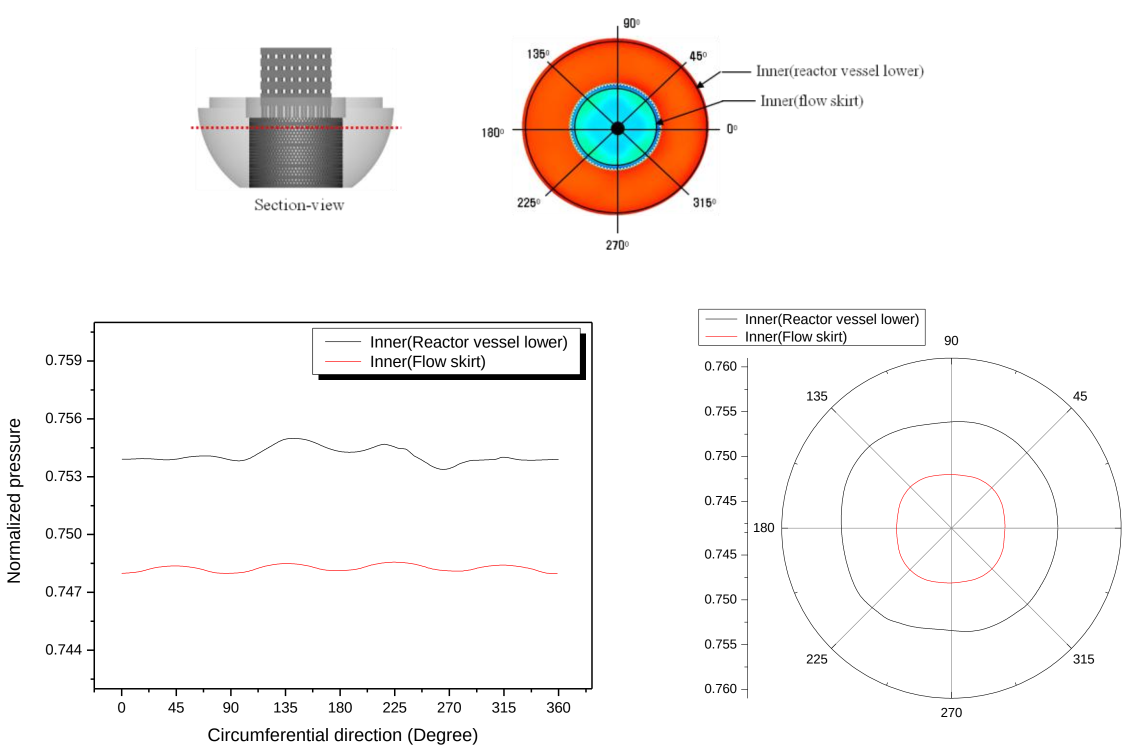

Figure 7 Pressure distribution in the circumferential direction of the reactor vessel lower and flow skirt

The circumferential pressure distribution difference of about 50 Pa occurs at the lower part of the reactor vessel, but the pressure distribution difference at the flow skirt was only about 10 Pa.
Figure 8 is the circumferential pressure distribution at the lower and upper wall of the upper guide structure. At the lower and upper part of the upper guide structure, the pressure distribution largely occurs with the measurement location due to the complicated flow path generated at the core part and the control rod protection tube. The fluid passed the core part showed a stagnation phenomenon near 45°, 135°, 225°, 315° location, and the pressure at these locations were high.
The uniformed fluid at the flow skirt fluctuates because of the complicated structure of the core and the fuel alignment plate. The circumferential pressure distribution difference generated at the lower part of the upper guide structure is about 300 Pa. At the upper part of the upper guide structure, the pressure distribution is locally high due to the 12 flow holes. The numbers of the flow holes are 12 at every 30° interval in the circumferential direction. The pressure distribution difference generated in the circumferential direction of the upper part at the upper guide structure is about 400 Pa. The flow holes of the upper guide structure are necessary to discharge the fluid to the exit, but those make the irregular flow field of the core support barrel assembly.

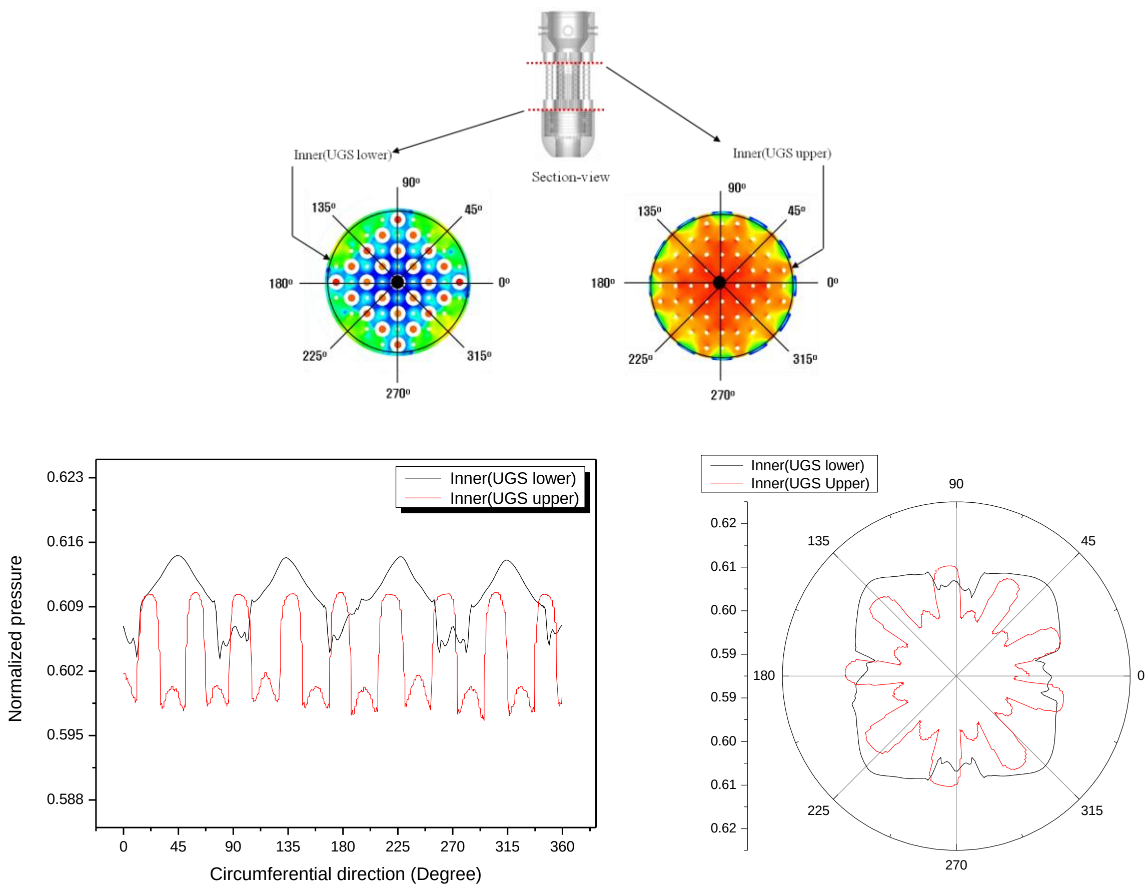

Figure 8 Pressure distribution in the circumferential direction of the upper guide structure lower and upper guide structure upper

Figure 9 is the circumferential pressure distribution formed at the lower, center, upper wall of the core support barrel. The lower part of the core support barrel has no flow holes from the upper guide structure assembly. Therefore, the lower area of the core support barrel shows a high-pressure. The pressure distribution difference generated at the circumferential direction of the lower part of the core support barrel was relatively small as about 10 Pa.

The central part of the core support barrel showed a high pressure due to the flow holes of the upper guide structure, and the pressure difference between flow hole area and no flow hole area is about 500 Pa. At the core support barrel, a local pressure distribution largely occurs due to the flow holes of the upper guide structure. The fluid discharged from the flow holes of the upper guide structure strongly collides to the wall of the core support barrel.

Most of the fluid flow through the pipe exit, but some fluid is congested at the upper part of the core support barrel. The pressure distribution difference generated in the circumferential direction is about 2 Pa, the flow field shows a uniform phenomenon in the entire area.

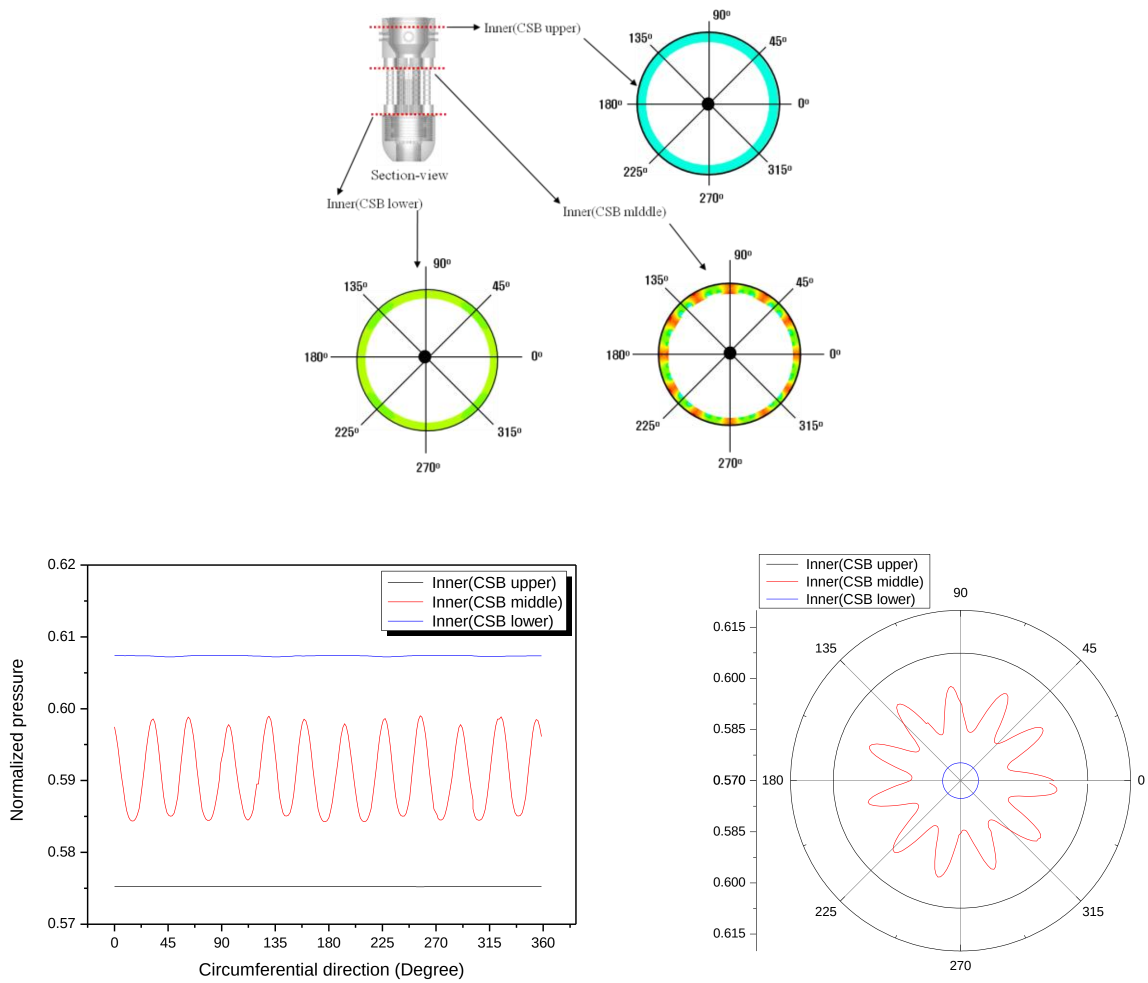

Figure 9 Pressure distribution in the circumferential direction of the core support barrel upper, core support barrel middle and core support barrel lower

4. Conclusion

In this study, flow analysis of the down-scaled model for SMART prototype was performed to analyze the flow-induced loads at the reactor internal structure and the main components. The axial pressure distribution of the flow analysis showed a similar tendency with the experimental data, the average error between the flow analysis and the experimental data appeared about 5% in most of area.

The circumferential pressure distribution showed an irregular phenomenon in most of areas due to the flow of the fluid. In particular, the circumferential pressure distribution of the core support barrel showed the most irregular phenomenon. The inside wall of the core support barrel showed the circumferential pressure distribution difference of 500 Pa because of the flow holes of the upper guide structure. The irregular pressure of 500 Pa is about 0.37% in comparison to the inlet pressure.

5. References

[1] M.J. Pettigrew, "Flow induced vibration ; recent findings and open questions", Nuclear engineering and design, Vol. 185, 1998, PP. 249-276.

[2] D.S. Weaver, "Flow induced vibrations in power and process plant components-progress and prospects", Journal of pressure vessel technology, Vol.122, 2000, PP. 339-348.

[3] Hyoung-Hee Cho, "Research on the estimation method for flow induced loads in reactor internals", KAERI-CM1182-2010, 2010, pp.5~7.

[4] Kyoung-Rean Kim, "Analysis for flow induced loads of the SMART reactor internals", KAERI-120-TC-013, 2010, pp.10~11

[5] Merle C. Potter and Midhat Hondzo, "Mechanics of fluids", Third edition, Prentice-Hall, Inc, California.